# Quantitative Surface-Enhanced Spectroscopy

Ryan D. Norton, Hoa T. Phan, Stephanie N. Gibbons, and Amanda J. Haes

Department of Chemistry, University of Iowa, Iowa City, USA, 52242; email: amanda-haes@uiowa.edu

Xxxx. Xxx. Xxx. Xxx. YYYY. AA:1-22 https://doi.org/10.1146/((please add article doi))

Copyright © YYYY by Annual Reviews. All rights reserved

## Keywords

SERS, intermolecular interactions, quantitative detection, surface selection rules

#### **Abstract**

Surface-enhanced Raman scattering (SERS), a powerful technique for trace molecular detection, depends on chemical and electromagnetic enhancements. While recent advancements in instrumentation and substrate design have expanded the utility, reproducibility, and quantitative capabilities of SERS, some challenges persist. In this review, advances in quantitative SERS detection are discussed as they related to intermolecular interactions, surface selection rules, and target molecule solubility and accessibility. After a brief introduction to Raman and SERS, impacts of surface selection rules and enhancement mechanisms are discussed as they relate to the observation of activation and deactivation of normal Raman modes in SERS. Next, experimental conditions that can be used to tune molecular affinity to and density near SERS substrates are summarized, and considerations while tuning these parameters conveyed. Finally, successful examples of quantitative SERS detection are discussed, and future opportunities are outlined.

Contents	
1. INTRODUCTION	2
1.1. Overview of Vibrational Spectroscopy	2
1.2. Correlating SERS Vibrational Modes to Functional Groups	3
1.3. Exploiting SERS Intensities for Quantification	4
1.4. Recent Progress in Quantitative SERS Detection	4
2. SELECTION RULES AND THE IDENTIFICATION OF VIBRATIONAL MODES	7
2.1. Group Theory and Vibrational Spectroscopy	7
2.2. Correlation of Enhancement Mechanisms to Vibrational Mode Symmetry	7
3. RELEVANCE OF MOLECULAR PROXIMITY TO AND DENSITY NEAR SERS SUBSTRATES	8
3.1. Molecular Affinity for and Proximity to SERS Substrates	9
3.2. Importance of Ions, Solvent, and Surfactants for SERS	11
3.3. Importance of Electric Field Strength and Gradient for Quantitative SERS	13
4. SUMMARY AND OUTLOOK	15

#### 1. INTRODUCTION

This review article explores how surface-enhanced Raman scattering (SERS) has been used for the the quantitative detection of small molecules. The article begins with a brief review of the fundamentals, then proceeds with our current understanding of SERS and recent progress towards reliable quantification of small molecules.

#### 1.1. Overview of Vibrational Spectroscopy

Vibrational spectra reveal unique information about chemical bonding as well as rotational and vibrational motion associated with molecules.(1) This information is obtained through the presence and location of observed spectral features. Infrared (IR) absorption and Raman scattering provide complimentary vibrational features, which depend on their selection rules.(2) While infrared spectroscopy relies on a change in dipole moment within a molecule, Raman scattering arises from changes in polarizability upon vibrational excitation. Although the probability of observing IR absorption is higher than that for Raman scattering, water absorption can limit aqueous IR measurements. As such, this review article focuses on Raman scattering and its potential applications for molecular quantification in aqueous solutions.

Raman scattering depends on a change in molecular polarizability as bond angle or length changes  $\left(\frac{\delta\alpha}{\delta Q}\right)$ .(1, 2) Vibrational spectroscopy originates from bond polarization induced by the oscillation of the incident electric field, and this induced polarization is described as a product of polarizability  $(\alpha)$  and the incident electric field (E):(2)

$$P = \alpha E = \left[\alpha_0 + \left(\frac{\delta \alpha}{\delta Q}\right)\right] \left[E_0 \cos(2\pi \bar{\nu}_0 t)\right]$$

$$= \alpha_0 E_0 \cos(2\pi \bar{\nu}_0 t) + E_0 Q \left(\frac{\delta \alpha}{\delta Q}\right) \frac{\cos(2\pi (\bar{\nu}_0 + \bar{\nu})t) + \cos(2\pi (\bar{\nu}_0 - \bar{\nu})t)}{2}$$
1.

The first term describes Rayleigh scattering while the following terms represent anti-Stokes at  $(\bar{\nu_0} + \bar{\nu})$  and Stokes scattering at  $(\bar{\nu_0} - \bar{\nu})$ . As such, Raman scattering depends on the

distortion of the electron cloud upon interaction with an applied electric field. Changes in molecular polarizability are realized through molecular vibrations allowing the electron clouds of each atom to vary in both relative distance and position. (1) Analyzing these spectra leads to the identification of specific vibrational modes assigned to unique changes in polarizability for functional groups. This identification process is the basis of chemical specific vibrational spectroscopy.

Raman scattering can be used to detect molecules based on observation of unique vibrational modes. As previously shown, Raman scattering is reported by calculating energy differences between incident and emitted photons. These quantized frequencies are distinct for each group of bonded atoms (i.e., functional group). Because each molecule contains a unique combination of different functional groups, resulting spectra contain distinguishable vibrational modes.(1) These vibrational spectra provide information that distinguishes chemicals by the absence or presence of unique vibrational features.

## 1.2. Correlating SERS Vibrational Modes to Functional Groups

Vibrational mode frequencies and band widths arising from ensemble-averaged measurements depend on the chemical properties of the molecules in the laser beam and the surrounding matrix.(1) Bond strength and polarizability govern the expected vibrational frequencies for a molecule or functional group.(2) While the amount of energy required to induce excited state oscillations can be modeled as a function of force constant and reduced mass, polarizability is an inherent property of a molecule or functional group that is dependent on its surroundings. Additionally, the band width of a given vibrational mode is typically quantified by its full-width at half maximum (FWHM) and is greatly affected by interactions between the environment and nearby functional groups.

Vibrational frequencies, which depend on the local environment, are different for Raman and surface-enhanced Raman scattering (SERS). The local environment of a molecule observed in Raman can be modeled in free space whereas molecules observed in SERS must include an interface, which induces a change in the electron density of that molecule.(3, 4) If a molecule contains an electron-rich functional group that has affinity for the metal, molecule-to-metal electron transfer between the metal and molecule decreases, which also decreases its electron density and bond strength. As a result, the vibrational frequency red-shifts in SERS vs. normal Raman scattering.

Vibrational band widths observed in SERS spectra are governed by the uncertainty principle and variations in intermolecular interactions as well as molecular orientation.(1) Band widths of ensemble averaged measurements, which can be quantified through FWHM, are limited by uncertainty.(5, 6) The FWHM of a vibrational feature can be quantified experimentally and related to the partial derivative of potential energy as a function of position. As a result, potential energy wells are used to describe vibrational motion/modes in terms of an anharmonic oscillator model, which is represented by Morse potential energy diagrams. The potential energy wells are used to describe the probability of finding an electron within a bond or, more generally, its local electron density.(1) Local electron density is expected to change with the presence and strength of intermolecular interactions, which depend on both the type of interactions as well as the orientation of the molecules probed. As intermolecular interactions increase in number and/or strength, the potential well flattens as the uncertainty of knowing electron position increases. This causes the potential well depth to decrease and the FWHM of a resulting vibrational frequency to increase.

## 1.3. Exploiting SERS Intensities for Quantification

The probability of detecting spectral features, which are described by Raman cross sections, increases as SERS intensities become distinguishable from noise. (7) Raman cross sections represent the ratio of scattered to incident photons. Thus, Raman-active vibrations arising from functional groups with larger scattering cross sections are more likely to be detected than those with smaller values. Raman cross sections can also be used to relate the amount of scattered light to the probability of a feature being detected. As the amount of scattered light increases, the probability of observing the relevant mode increases assuming noise is constant.

Chemical enhancement mechanisms, including ground state, charge-transfer, and resonance Raman enhancements, are short range effects (less than 1 nm) that lead to an increase in Raman signals by 100-10,000 times.(7, 8, 9) (**Figure 1a**) While smaller in magnitude than electromagnetic enhancement, these effects are very short range (typically on the Angstrom level). Ground state chemical enhancement does not require the formation of new electronic states to arise between the substrate and molecule. The most common chemical enhancement mechanism is through charge-transfer in which a metal-molecule charge transfer state is induced when the metal and molecule interact at short distances. If the incident photons are in resonance with this new charge transfer state, resonance Raman enhancement occurs.(8)

Electromagnetic enhancements further increase Raman signals by 6-8 orders of magnitude and depend on the induced electric fields resulting from plasmon excitation.(7) The electromagnetic enhancement arises when molecules are placed in an induced electric field near a SERS substrate. The magnitude and direction of this field play direct roles in determining the extent of signal enhancement.(7) Typical electromagnetic enhancements are considered to be long-range (1-10 nm from a surface) and decay quickly as the distance between the analyte and metal surface increases.(7, 10)

### 1.4. Recent Progress in Quantitative SERS Detection

Recent efforts in promoting quantitative SERS detection focus on controlling and or maximizing electromagnetic enhancement through substrate design, improving selectivity of analyte binding to the substrate, and/or accurately identifying vibrational bands. Quantitative detection can be achieved when plasmonic enhancement is preserved, an effect typically achieved by preserving the composition, shape, and size of SERS substrates.(11, 12) Surface modification is often key as chemical or physical changes associated with the substrate must be minimized, or internal standards must be used to correct for variations in the resulting induced electric field.(13, 14, 15, 16, 14) Additionally, functional groups on SERS substrates can be introduced to increase selective interactions with the molecule of interest thus reducing the spatial fluctuations of SERS intensities, but this surface chemistry increases the distance between the SERS substrate and chromophore.(17, 18) This has the unintended consequence of reducing SERS intensities.

Improving the plasmonic stability of SERS substrates leads to reproducible measurements assuming the molecule interacts with the substrate at short distances. This approach preserves the induced electric field that molecules experience near a nanostructured surface thus enabling a direct correlation between SERS intensity and molecular concentration. (12, 19, 20) Microporous silica membranes, for example, were shown to effectively minimize impacts from collisions between solution-phase nanoparticles,

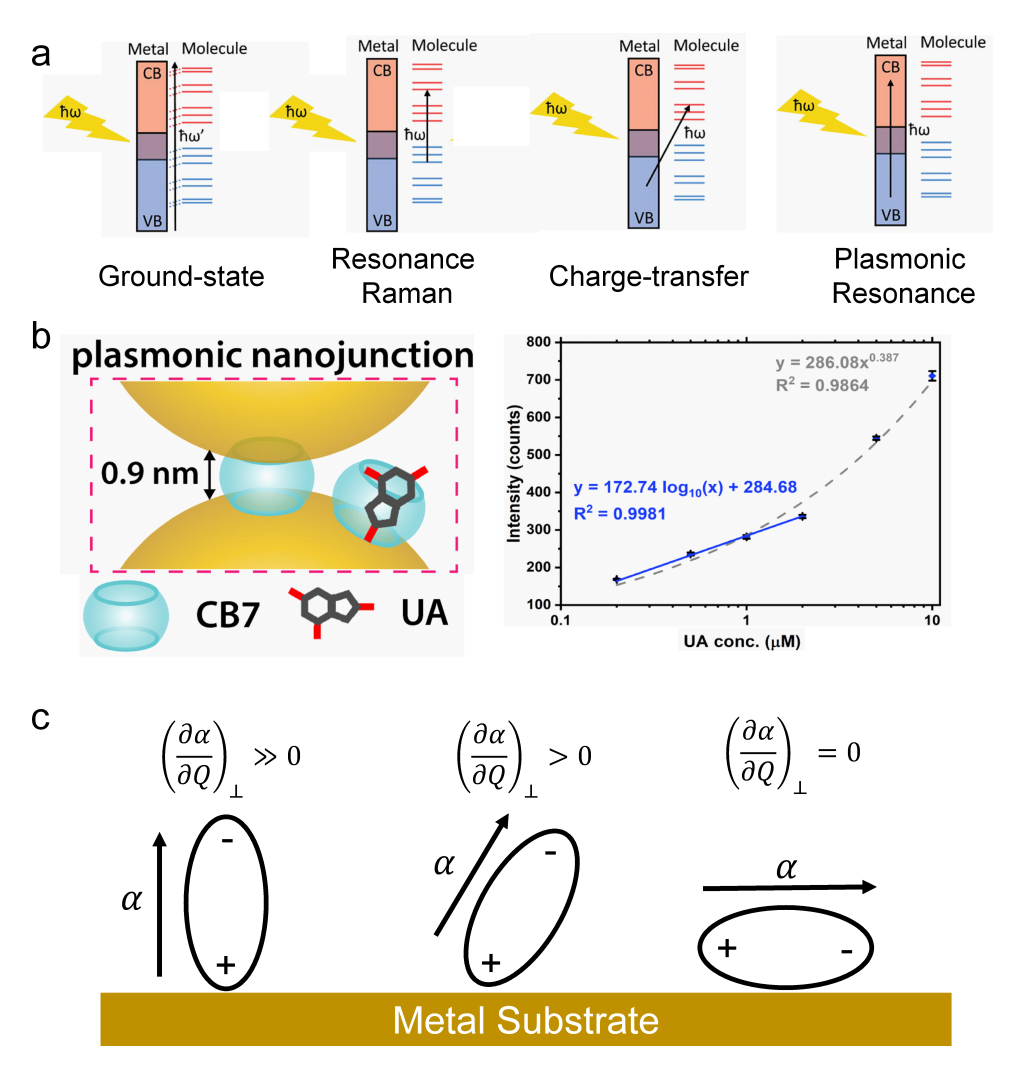


Figure 1

(a) Enhancement mechanisms associated with SERS. Panel a adapted from Reference 8; copyright 2020 American Institute of Physics. (b) An example of a plasmonic nanojunction where aggregation is mediated by an empty cucurbit[7]uril (CB7) while uric acid (UA) is enriched on the surface of Au nanoparticles via host-guest complexation (left) and a correlation between SERS intensity at skeletal ring deformation mode (640 cm<sup>-1</sup>) as a function of UA concentration (right). Panel b adapted from Reference 17; copyright 2020 MyJove Corp.(c) Illustration of surface selection rules

and electromagnetic coupling between nanoparticles was approximately constant and molecules could diffuse through small, sub-2 nm diameter nanopores for quantitative SERS enhancements.(21, 22, 23) Because SERS intensity depended on the molecules instead of variations in the plasmonic properties of the SERS substrates, the kinetics and thermodynamics of adsorption, structural rearrangements, and protonation states of molecules were successfully investigated. SERS substrates functionalized by polymers(24) and proteins(25)

were also utilized to prevent solution-phase nanoparticle aggregation thus facilitating quantitative SERS detection.

Using internal standards facilitate SERS-based quantification even when the induced electric fields near SERS substrates vary. (13, 14, 15, 16) The internal standard should possess a similar affinity to the plasmonic surface as and a similar Raman cross-section to the analyte to prevent competitive adsorption and so that similar dynamic ranges for quantification are possible. (14, 26) Additionally, ensuring that the internal standard and target molecule experience similar or predictable electromagnetic enhancement increases the likelihood that relative SERS intensities can be used for quantification. (26) 2-Naphthalenethiol, for example, was used as an internal standard in the SERS detection of 4-nitrothiophenol using silver nanoparticles. (13) The internal standard was engineered to be inside the silver nanostructures while the analyte adsorbed to the exterior of these nanostructures. Unique ring stretching modes from both molecules were observed in SERS spectra, and the ratio of analyte-to-internal standard intensities was used to quantify 4-nitrothiophenol. Because the analyte induced nanoparticle aggregation, slight changes in the plasmon resonance of these nanostructures arose but could be tolerated in the assay as the relative ratio remained correlated to analyte concentration thus facilitating successful quantification. Another example of successful quantification using internal standards was achieved for the quantification of 4-mercaptobenzoic acid. In this study, 1,4-benzenedithiol was used as an internal standard and cellulose filter paper containing silver nanoparticles was used to maximize quantification. (14) This SERS assay was, in part, successful because the use of internal standard caused the relative standard deviation of SERS intensities for 4-mercaptobenzoic acid across the filter paper to impressively decrease from 53% to 11%. In both of these cases, internal standards promoted quantitative SERS detection by correcting for changes in both chemical and plasmonic variations in the sampling volume.

Minimizing impacts of electric field variations near SERS substrates promote quantitative SERS detection. For instance, surface modification (17, 18) can be employed to simultaneously facilitate interactions between target molecules and SERS substrate while also maintaining the analyte-to-surface distance. One successful example of this mechanism to maximize quantitative SERS detection involved cucurbit[7]uril (CB7) to selectively capture uric acid via host-guest complexation as shown in (Figure 1b).(17) Given this selective chemistry, SERS from uric acid immobilized inside CB7 was observed rather than from molecules in solution. CB7 also induced the formation of precise plasmonic junctions between gold nanostructures, which induced a strong and stable electric field and consequently, quantitative SERS intensities for uric acid. A second example of quantitative SERS detection utilized an electrochemically assisted platform to promote molecular adsorption. (18) The SERS substrate consisted of Au-capped silicon nanopillars on a silica wafer, which was negatively charged and served as a working electrode, and the electrochemical potential was varied to facilitate the adsorption of positively charged melamine at pH 3.6. Quantitative SERS detection was only observed at negative potentials where electrostatic attraction between positively charged melamine and the SERS substrate was achieved. This method was also successful in complex matrices such as milk, which further expanded the powerfulness of this quantitative SERS platform.

## 2. SELECTION RULES AND THE IDENTIFICATION OF VIBRATIONAL MODES

Group theory and surface selection rules can be used to predict the presence and enhancements of vibrational modes observed in a SERS spectrum, respectively. (27, 28) Group theory utilizes matrices to represent a molecule and its spatial orientation thus providing a physical description for molecular vibrations. (28) Once a vibrational mode is identified, surface selection rules provide a spatial representation given by group theory to correlate the polarizability tensor with respect to the induced electric field from plasmon excitation. (27) In this section, correlations between group theory and vibrational spectroscopy, and enhancement mechanisms and vibrational mode symmetry are discussed.

## 2.1. Group Theory and Vibrational Spectroscopy

Matrices simplify a point group in the form of a character table thus facilitating the straightforward identification of Raman-active modes. In group theory, every point group has a specific character table that summarizes each symmetry operator and active vibrational mode.(28) Each character table is composed of matrices representing the movement of atoms upon application of a symmetry operator. Character tables display well organized information about symmetry and Raman activity of each vibrational mode.

Point groups categorize molecular structure by symmetry and mathematically describe how molecular orbitals change during vibrations. Every molecule is sorted through a systematic process following the absence or presence of symmetry in a specific order of molecular structure, rotation axes, reflection planes, then complex symmetry. (28) Grouping molecules leads to the utilization of a character table for each group thus distinguishing vibrational similarities between molecules. Vibrational motion associated with any molecule can be understood through the use of point groups and symmetry operators.

Symmetry operators are used to derive irreducible representations in a character table for determining Raman-active modes. These operators include molecular rotations, reflections, inversions, as well as a combination of these. Irreducible representations are derived from reducible representations, which are matrices representing the movement of atoms after applying a symmetry operator. Each character table contains linear and non-linear functions to describe the activity of each irreducible representation. The functions describe combinations of symmetry operators that abide by a specific irreducible representation. Linear functions in character tables are IR-allowed whereas non-linear functions are associated with Raman-allowed modes. (28)

#### 2.2. Correlation of Enhancement Mechanisms to Vibrational Mode Symmetry

Irreducible representations describe the local symmetry of a functional group near SERS substrates. (28) Irreducible representations can be utilized to describe the orientation of a molecule or specific vibration mode in space with respect to an interface. Because electromagnetic enhancement depends on the magnitude and direction of the induced electric field, largest enhancements arise from the parallel alignment between the induced electric field and vibrational motion. Enhancement decreases as the angle between the induced electric field and vibration increases until these vectors are perpendicular. This is the basis of surface selection rules for SERS (Figure 1c).

The local symmetry of functional groups can change upon interaction with an inter-

face, which subsequently and selectively activates or deactivates vibrational modes. These changes are predicted using surface selection rules. (28, 29) When a molecule interacts with a SERS substrate, the symmetry operators applicable to the molecule can change because of variations in its local symmetry. Both the formation of a new bond or changes in local electron density, which leads to a distortion in intramolecular structure, can arise. As such, polarizability can vary thus impacting the observation of vibrational modes in SERS spectra. If these substrate interactions cause the polarizability vector to be parallel to the plasmon induced electric field, SERS intensities are often maximized. (29) Alternatively, perpendicular orientation of these would lead to the absence of a feature. (27) As a result, surface selection rules can be used to understand and predict the absence or presence of various vibrational modes in a SERS spectrum.

Chemical enhancement mechanisms typically promote the enhancement of asymmetric modes due to symmetry changes induced from direct or short-range interactions with an interface. (8, 9, 30) The activation of asymmetric modes is highly dependent on variations in the electron density of a molecule upon interaction with a metal. (22, 31) The asymmetric stretching mode of an aromatic ring, for instance, can be activated upon initial adsorption to gold. (22, 31) Increasing the packing density of the monolayer causes the  $\pi$  electrons in the aromatic rings to become delocalized, which causes the asymmetric stretching mode to decrease. A similar phenomenon was observed when the enhancement of asymmetric stretching modes for sulfonate was promoted when one of the nitrogen atoms in the Good's buffer HEPES became deprotonated and the relative electron density in sulfonate increased. (32) Both of these examples illustrate the impacts of short range interactions and chemical enhancement of asymmetric vibrational modes.

Highly symmetric vibrations are typically enhanced electromagnetically. (28, 33) This enhancement mechanism depends on surface selection rules and the alignment between the polarizability and induced electric field vectors. When the change in polarizability is largest and the vectors are aligned, SERS intensities of symmetric stretching modes can be combined with out-of-plane bending modes to determine the orientation of molecules at the metal interface. (34)

Finally, the intensity of a vibrational mode observed in SERS depends on the magnitude of the induced electric field of both the substrate and analyte as well as the direction and magnitude of the polarizability tensor. Namely, the SERS intensity is approximately proportional to the electric field to the fourth power, or more precisely to the square of the plasmon induced electric field multiplied by the square of that from the molecule. Once the local symmetry of a functional group is determined with respect to an enhancing surface, the observation of the resulting modes depends on vector alignment and both chemical and electromagnetic enhancement mechanisms.

## 3. RELEVANCE OF MOLECULAR PROXIMITY TO AND DENSITY NEAR SERS SUBSTRATES

Ensemble-averaged SERS intensities scale with the number of molecules in the induced electric field and not on the analyte concentration added to solution. While surface selection rules previously suggest that the SERS effect is maximized when the polarizability  $(\vec{\alpha})$  and induced electric field  $(\vec{E})$  are parallel, SERS intensity also depends on  $|E_{surface}|^2$ , which varies with analyte-to-surface separation distance, and the number of molecules that experience the induced electric field.(35, 36) As such, high molecular density and their close

proximity to the metal interface promotes quantitative SERS detection. In this section; impacts of ions, solvent, and surfactants on quantitative SERS detection are evaluated.

## 3.1. Molecular Affinity for and Proximity to SERS Substrates

Surface stabilizers can either block or promote SERS activity depending on steric effects and/or relative binding affinities. For solution-phase SERS substrates, stabilizing agents are often employed to reduce surface energy through promotion of elastic, electrostatic, and osmotic forces. Thus, the physical stability of these nanomaterials can be varied by using different stabilizing agents. Bulky polymers such as polyvinylpyrrolidone, (37) polyethylene glycol,(38) or proteins(39)) increase repulsive steric interactions between nanostructures upon collision thereby facilitating the suspension of nanoparticles in both organic and biological environments. Interactions between analytes and these steric barriers, however, can potentially prevent analytes from being detected using SERS because of their density which can block molecular diffusion and/or their thickness which occupies volumes associated with the highest electric fields.(11) Ionic stabilizing agents such as citrate(40, 41) or HEPES(42), promote the physical stability of solution-phase nanoparticles through electrostatic repulsive forces. These stabilizing agents can be used to overcome the distance dependence limitations associated with thick steric barriers. In addition, target molecules can either undergo intermolecular interactions with functional groups associated with the stabilizing agents (41) or displace them. (40) These examples emphasize the importance of surface chemistry as well as molecular affinity for and proximity to a substrate for promoting SERS quantification.

Molecules that directly bind to SERS substrates experience the largest induced electric fields and are more likely to be detected than those farther away from the SERS interface. Functional groups containing S, O, and N atoms were previously shown to have high binding affinities for metal surfaces,(43, 44) so molecules possessing functional groups contain these often displace surface stabilizers and directly adsorb to SERS substrates. Examples of analytes that can directly bind to Ag and Au SERS substrates are shown in (**Figure 2a**). Thiol groups, for example, commonly adsorb to plasmonic metallic surfaces for SERS detection because of their high binding energy (~40 kcal/mol) to gold surfaces.(45) Thiols have been shown to displace a wide range of stabilizing agents including citrate,(40) HEPES,(42) EPPS,(46) or polyvinylpyrrolidone(47) by directly binding to a metal. This allows target molecules to be easily detected because of maximized chemical and electromagnetic enhancements.

Previously, 2-naphthalenethiol(48) was detected at low micromolar concentrations by displacing citrate on gold nanospheres. As distance between the analyte and surface increases, however, SERS intensities decrease because of the decaying electric field. An example of SERS distance dependence was illustrated when gold nanospheres encapsulated by microporous silica shells with thicknesses varying from 1.7 to 14.5 nm were used for the detection of 2-naphthalenethiol.(10) As the silica thickness increased, SERS intensity at 1380 cm<sup>-1</sup> ( $\nu_{CC}$ /C-C symmetric stretching) decreased rapidly, and the molecule became undetectable once the silica shell exceeded 4 nm thus emphasizing the importance of the distance between the analyte and SERS substrate.

The direct and spontaneous binding of a monolayer of ligands results in the formation of self-assembled monolayers (SAMs) where ligand density and intermolecular interactions influence their orientation with respect to the surface normal, and consequently, the po-

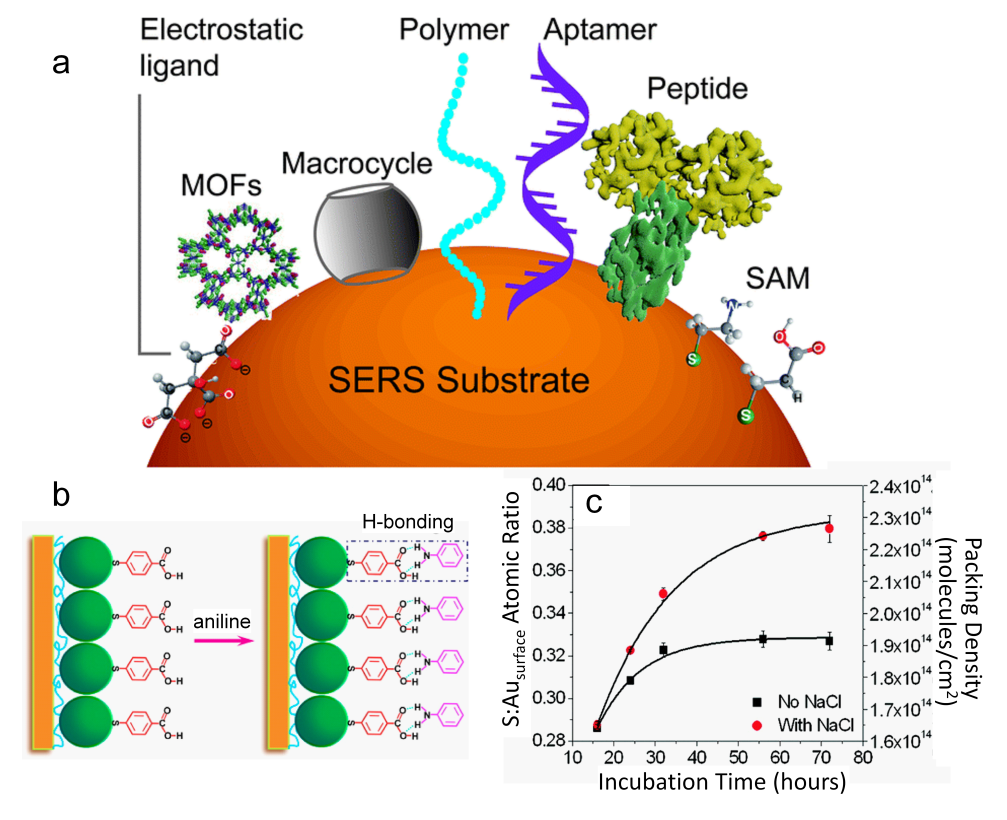


Figure 2

(a) Cartoon of various surface-affinity ligands, which can immobilize target molecules through physisorption, chemisorption, electrostatics, molecular sieving effects using porous materials such as metal organic frameworks (MOFs), host-guest recognition using macrocycles or molecular imprinted polymers, biological recognition using DNA or peptides, and chemical derivatization using self assembled monolayers (SAMs). Panel a adapted from Reference 44; copyright 2021 Royal Society of Chemistry. (b) Illustration of the Formation of the Ag nanoparticles/mercaptobenzoic acid/aniline. Panel b adapted with permission from Reference 51; copyright 2014 American Chemical Society. (c) Comparison of the S:Au surface ratio (left-hand y axis) and packing density (right-hand y axis) vs incubation time for thioctic acid functionalized gold nanospheres prepared in the presence and absence of NaCl. The solid lines represent exponential fits for the S:Au<sub>surface</sub> atomic ratio vs incubation time. Panel c adapted with permission from Reference 84; copyright 2011 American Chemical Society.

larizability vectors associated with their vibrational modes. Electrostatic repulsive forces between terminal groups were shown to impact the tilt angle of thiophenol and its derivatives on metals.(22, 34) At equilibrium, p-aminothiophenol and 4-mercaptobenzoic acid have tilt angles of 33 and 44° while thiophenol lies in a nearly parallel orientation with respect to the surface normal.(34) As this tilt angle increases, the intensity of the C-H in-plane bending mode decreases as its polarizability vector becomes orthogonal to the induced electric field. Opposite trends are observed for the C-H and C-C-C out-of-plane bending modes as their polarizability vectors are initially perpendicular to the induced electric field and then become oriented in a parallel manner. In alkanethiol SAMs, van der Waals attractive forces

between adjacent alkyl chains influence the tilt angle of molecules. (49) As the length of the alkyl chain increases from 2 to 11 carbons, increasing van der Waals forces causes the tilt angle relative to the surface normal to decrease. This causes the C-C symmetric stretch as well as the CH<sub>2</sub> wagging and deformation vibrations from longer aminoalkanethiols to be observed. In contrast, vibrational modes arising from amines were detected in SERS spectra of the shorter SAMs. This is yet another example of factors that need to be considered when pursuing quantitative SERS detection.

Molecules with poor affinity to SERS substrates can be detected via initial surface modification, which can subsequently be used to increase the dwell time of molecules in a plasmon induced electric field via a wide range of intermolecular interactions including electrostatics, (50) hydrogen bonding, (51) van der Waals forces, (52) and covalent bond formation. (53) Surface modification commonly utilizes thiols, which contain an additional functional group that is capable of inducing intermolecular interactions with target molecules. This, however, increases the distance between the chromophore and SERS substrate and weakens the observed SERS intensities. 4-Mercaptobenzoic acid, for example, formed a SAM on silver nanoparticles. Aniline was subsequently detected via hydrogen bond formation with the terminal carboxylate groups as illustrated in (Figure 2b). (51)

Evidence of aniline detection was apparent from changes in SERS features associated with 4-mercaptobenzoic acid. Vibrational modes that are sensitive to hydrogen bond formation were most impacted. In addition, interactions between the carboxylic acid (electron withdrawing) and amine (electron rich) groups increased the polarizability of C-C, C-H, and C-S bonds in 4-mercaptobenzoic acid thus influencing their SERS intensities. As aniline concentration increased, intensities for the in-plane ring breathing (1022 and 998 cm<sup>-1</sup>), C-H out-of-plane deformation (691 cm<sup>-1</sup>), and C-S symmetric stretching (417 cm<sup>-1</sup>) modes increased. Another example in which a carboxylate group promoted quantitative SERS detection is through uranyl coordination. Uranyl has poor affinity to gold but is readily detected using to SERS substrates containing SAMs with terminal carboxylate groups. (53, 54, 55) The Gibbs free energy associated with uranyl coordination to carboxylate was approximately 8 kcal/mol.(53) The quantitative SERS signals associated with uranyl detection, however, also depends on SAM thickness. As the alkanethiol chain length increased from 3 to 11 carbon atoms, saturated SERS intensities associated with  $\nu_{UO_2}$  decreased by a factor of 8. These examples further emphasize the importance of the proximity of the chromophore and relative affinity between the target molecules and SERS substrates.

### 3.2. Importance of Ions, Solvent, and Surfactants for SERS

SERS detection depends on the solubility of the target molecule in its initial phase. For instance, parameters that promote molecular dissolution in a solvent ultimately increases its detectability. As discussed in the previous section, SERS signals are typically maximized when molecules experience the largest electric field strength near a SERS substrate. Thus, molecular and SERS substrate solvation must be considered. Because target molecules can contain polar and/or non-polar functional groups, an ideal solvent or solvent mixture should possess a similar degree of polarity as the analyte to maximize its solubility. Organic compounds such as benzene(32), benzene derivatives,(56) and 2-naphthalenethiol,(40, 48) are non-polar and poorly soluble in water. To promote their detection in aqueous solutions, these compounds can be initially solubilized using low polarity solvents (i.e., alcohols,(32, 40) acetone,(57) or acetonitrile(58)) before adding them to water.

Protonation can also influence the dissolution and SERS detection of molecules. (59, 60) For example, the addition of an acid or a base was found to protonate secondary amines and deprotonate carboxylic acid groups, respectively, in ciprofloxacin. By adjusting the protonation state of the molecule, dissolution and SERS detection in an aqueous environment were promoted. (60) Acidification (pH<7) also favored SERS detection of uranyl hydroxide complexes, which are more soluble in acids vs. bases. (54, 59) As such, solvents and pH play an important role in promoting dissolution of analytes thus increasing the likelihood of detecting molecules using SERS.

The surface reactivity of a nanostructure, which includes but is not limited to dissolution, oxidation, ripening, and aggregation/agglomeration, needs to be considered for selecting experimental conditions for quantitative SERS measurements. Typically, nanoparticles exhibit high surface energies and chemical potentials relative to bulk materials because of the large number of surface to total atoms. As a result, nanostructures more readily undergo dissolution in acidic solution relative to bulk materials.(61, 62, 63) Additionally, aromatic thiols suspended in hexane were shown to promote metal dissolution through the formation of Au(thiol)<sub>2</sub> compounds, which were thermodynamically favored over Au atoms or clusters.(64)

The solubility of oxygen varies with solvent composition (65, 66). As a result, metal oxidation is impacted (i.e., Ag(67, 68) and Cu(69)) as is the affinity between the SERS substrate and SERS chromophore. At standard pressure and temperature, oxygen is most soluble in water and alkanes, then in alcohols and aromatic solvents. As the alkyl chain length increases, oxygen solubility increases in alcohols but decreases in alkanes. Furthermore, the presence of protons,(32, 70) halides,(32, 71, 72, 73) salts,(74, 75) and solvents(76, 77) can weaken the affinity of surface stabilizing agents. One potential consequence of weakening interactions between stabilizing agents and a SERS substrate are morphological transformations of high surface energy nanostructures through surface atom migration or dissolution. Thus, the plasmonic properties of SERS substrates can vary thereby influencing quantitative SERS measurements.

Relative molecular affinities to SERS substrates compared to ions, solvent, and/or surfactants, govern surface accessibility and as a result, SERS activity. Halide anions, which have strong affinity to metal surfaces,(73) often have weaker or comparable binding energies to SERS substrates as SERS chromophores. If halides bind, the surface density of target molecules can decrease, which negatively impacts quantitative SERS detection. Increasing the concentration of chloride in solution reduced the adsorption of flumetsulam(78) and biotin(79) to gold leading to a decrease in SERS intensities for both molecules. At the highest chloride concentrations, no analyte was detected at the interface because the surface was saturated by chloride. The same effect was observed for surfactant-stabilized nanoparticles in which a surfactant bilayer prevented target molecules from diffusing near the metal interface for SERS detection.(80, 81) CTAB bilayers, for example blocked the binding and SERS detection of 4-mercaptopyridine onto gold nanorods suspended in water as the surfactant bilayer formed a steric barrier that inhibited ligand exchange and minimized SERS activity. When the CTAB bilayer was disrupted by the addition of acetonitrile, the molecule was readily detected as it was able to bind to gold.(82).

Solvents can also impact the surface accessibility of SERS chromophores with weak affinities for metals. (58) Methanol and acetone were shown, for example, to compete with copper phthalocyanide (CuPc) adsorption to silver. While acetone and methanol bind to silver through oxygen leading to a  $\nu_{C=O}$  mode, CuPc formed an induced dipole-induced

dipole interaction with silver via its aromatic ring resulting in the appearance of  $\beta_{C-H}$  (C-H bending mode). Furthermore, the lone pair electrons of the oxygen atom in acetone formed a stronger interaction to silver vs. methanol, so the adsorption rate of CuPc was slower in acetone vs. methanol. This suggests that solvents influence surface accessibility of SERS chromophores.

Finally, electrostatic interfacial energies, which depend on ion composition and concentration, can be minimized to increase molecular density near the metal interface and increase SERS intensities. Previous studies showed that the electrostatic interfacial energies  $(E^{EL})$  between two point charges are inversely proportional to the ionic strength of the solution.(83, 84) As ionic strength increases, shielding effects cause  $E^{EL}$  to decrease leading to an increase in molecular surface density. This was demonstrated for the adsorption of thioctic acid to gold in the presence of NaCl.(84) The zeta potential of thioctic acid functionalized gold nanospheres was less negative when the SAM formed in the presence of NaCl. X-ray photoelectron spectroscopy (XPS) results (**Figure 2c**) showed that the ratio of sulfur (S) to Au increased suggesting that the packing density of thioctic acid had increased, an effect that was attributed to shielding. The same effect was observed with thiolated DNA on gold surface but was attributed to charge shielding along the charged DNA backbone.(85) All examples in this section emphasize that ions, solvent, and surfactants must be considered when designing quantitative SERS assays.

## 3.3. Importance of Electric Field Strength and Gradient for Quantitative SERS

SERS intensities depend on electromagnetic coupling between plasmonic nanostructures and as a result, the induced electric field magnitude and its gradient. When the induced electric field varies over the length of a bond, electric field gradient effects rather than polarizability gradients govern Raman and SERS selection rules. While electromagnetically isolated nanospheres exhibit an induced but relatively weak electric field, electromagnetic coupling between two slightly separated nanospheres induces a strong electric field at the junction. (86, 87) A non-uniform distribution in induced electric field for anisotropic nanostructures where the strongest field extends from the features with the smallest radius of curvature. (88) These fields are often exploited in single molecule detection where SERS intensities depend on the relative position of the chromophore in the field. The variations are averaged out in ensemble-averaged measurements because fluctuations in the induced electric field are averaged out.

SERS intensities are inversely proportional to distance because of the rapid decay of the electric field. (10, 89, 90) Previously, SERS intensity was shown to be proportional to  $|E_{surface}|^2$ , which decreases as a distance from an interface increases. This correlation is described as follows: (10)

$$\mid E_T \mid \propto E_0 \left(\frac{r+T}{r}\right)^{-10}$$
 2.

where  $E_0$  is the induced electric field at the metal interface, r is radius of curvature, and T is the distance between the metal interface and the point where  $|E_T|$  is evaluated. This SERS distance dependence was illustrated for single-strand DNA detection using gold nanospheres.(90) As the number of adenine bases repeated in the strand increased from 2 to 18, the distance between terminal fluorescein and gold increased from 5 to 16 nm causing the intensities at  $\beta_{C-CH}$  (from fluorescein dye) and  $\nu_{CC,ring}$  (from adenine) to decrease

following equation 2. A similar phenomenon was observed in the SERS detection of uranyl where gold nanostars functionalized with mercaptoalkanoates containing 3 to 11 carbons were used. (53) As the chain length increased, the SERS intensity for uranyl ( $\nu_{UO_2}$ ) scaled with uranyl concentration as well as SAM thickness.

Quantitative SERS is promoted when "warm" SERS effects are exploited. For instance, steric barriers can be used to minimize electromagnetic coupling between nanostructures and also reduce the electric field strengths at nanostructured interfaces. Electromagnetic coupling is observed when the distance between two metal surfaces is less than two times that of the nanostructure decay length (i.e., the distance away from a surface where the electric field decreases by e (Euler's number)).(91, 92) As the separation distance between metal nanoparticles decrease, the strength of the induced electric field increases exponentially before reaching a maximum value (i.e., hot spot).(91) When a sub-nanometer gap is achieved, quantum tunneling diminishes SERS intensities of molecules present at these junctions. (93) Because nanoscale variations in inter-nanoparticle distances influence field strength, (94) quantitative detection is often limited. To overcome these challenges, "warm" spots where the distance between metal interfaces is larger than two times the nanostructure decay length can be introduced using well-controlled steric barriers. (21, 95, 96) Microporous silica membranes, for example, effectively minimized electromagnetic coupling between plasmonic nanostructures when shell thickness is greater the decay length of plasmonic nanoparticles. (97) Because nanopores in these membranes allowed small molecules to diffuse inside the silica membranes to the metal cores, quantitative SERS measurements were facilitated. Other examples involving silica shells (98, 99) and bulky polymers (100, 101) have also been used for molecular quantification using SERS. Successful quantification was facilitated by immobilizing SERS-active reporter molecules on the metal before shell encapsulation. This indirect SERS approach expanded the utility of SERS detection to include molecules with small Raman cross sections and improved the robustness of the nanostructures by maximizing their chemical and physical stabilities (Figure 3a).

Repulsive electrostatic forces between nanostructures helps preserve the induced electric field strength thus promoting quantitative SERS detection. These long range repulsive interactions(11, 46) can be achieved by manipulating the protonation states of functional groups on nanoparticle surfaces through pH variations (**Figure 3b**).(102, 103, 104) For example, gold nanospheres functionalized with 4-mercaptobenzoic acid remained plasmonically stable at pH 7, while experiencing electromagnetic coupling at pH 5(102) as the carboxylic acid groups became protonated around their pK<sub>s,surface</sub>. The same trend occurred with gold nanospheres functionalized with 11-mercaptoundecanoic acid (pK<sub>s,surface</sub>=4).(103) These nanospheres underwent electromagnetic coupling and aggregation below its pK<sub>s,surface</sub>. These examples emphasize the importance of plasmonic stability for facilitating quantitative SERS detection.

Solution-phase nanoparticle aggregates facilitate quantitative SERS detection when loosely packed because of "warm" SERS effects. To exploit these effects, the dynamics and kinetics of plasmonic nanoparticle cluster formation can be considered.(75, 78) Diffusion-limited cluster formation was found to preserve the induced electric field strengths because dense SAMs formed quickly(40) and diffuse clusters with large interparticle spacing was observed.(105, 106) In this limit, SERS intensities scaled with nanosphere concentration and diameter as long as plasmonic losses were minimized (**Figure 3c and 3d**). When cluster dynamics were considered, SERS substrates exhibited warm and uniform electric fields that could be exploited for quantitative SERS detection.

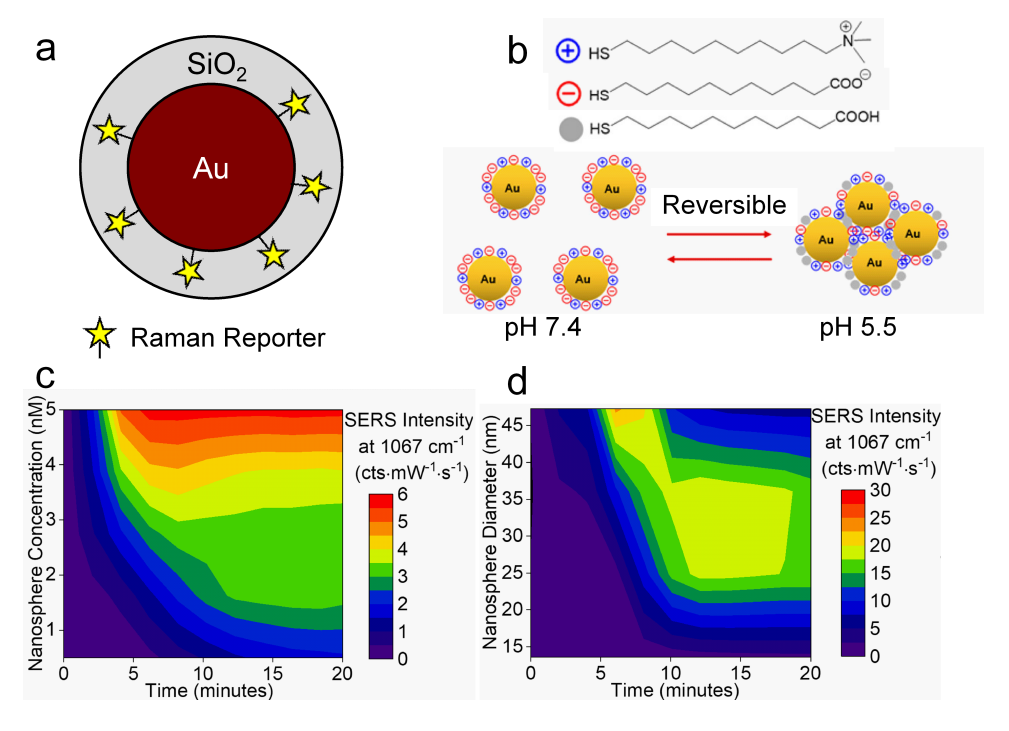


Figure 3

(a) Silica-coated gold nanoparticles with Raman reporters embedded at the core-shell boundary. Panel a adapted from Reference 98; copyright 2003 American Chemical Society. (b) The surface charge of gold nanoparticles is designed to be neutralized owing to the protonation of 11-mercaptoundecanoic acid (MUA) under the mildly acidic conditions. Panel b adapted from Reference 104; copyright 2017 American Chemical Society. (c) SERS intensity at 1067 cm<sup>-1</sup> as a function of nanoparticle concentration and (d) as a function of nanosphere diameter. SERS experimental conditions:  $\lambda_{\rm ex}=785$  nm,  $t_{\rm int}=20$  sec,  $P_{\rm laser}=83.3$  mW. Panels c and d adapted from Reference 40; copyright 2020 American Chemical Society.

## 4. SUMMARY AND OUTLOOK

Quantitative SERS detection requires accurate identification of vibrational modes from target molecules that are located near plasmonic substrates which induce reliable electric fields. Understanding the origins of vibrational modes and correlating these to SERS enhancement mechanism and vibrational frequency facilitates accurate predictions and assignments of SERS spectral features. The probability of detecting a molecule using SERS increases if its exhibits appreciable affinity to the enhancing substrate and if the number of molecules at that interface is maximized. This can be tuned by varying the composition of ions, solvents, and surfactants present in solution. SERS quantification is further promoted if the enhancing substrate is both chemically and physically stable.

From our discussions, we propose three opportunities to further improve the capabilities of quantitative SERS detection. First, silica encapsulation of plasmonic nanostructures with small radius of curvature features and large plasmonic fields(107) could be synthesized. Gold nanostars are one excellent candidate. These structures have been successfully synthesized for indirect SERS assays and through careful silica engineering.(108, 109) These structures,

however, have not reached their full potential due to limitations in morphology tuning(110) and subsequent SERS assay development.

Second, exploiting single nanoparticles for better understanding field gradient effects could be utilized. Theory suggests that field gradients are small near nanospheres(111) and significant near small radius of curvature features such as at the end of a nanorod.(107, 112) The dependence of SERS intensity on the position and orientation of the Raman chromophore in the field gradient could assist in understanding SERS quantification under these conditions.

Finally, impacts of molecular diffusion and affinity to the metal surface on quantitative SERS detection could be investigated under reaction-limited conditions, where cluster formation relies on the kinetics of molecular adsorption and flux.(106) Because the resulting clusters are typically closely spaced, methods to better control gap spacing between nanostructures could be used to further promote quantitative SERS detection using solution-phase nanostructures.

#### **DISCLOSURE STATEMENT**

The authors are not aware of any affiliations, memberships, funding, or financial holdings that might be perceived as affecting the objectivity of this review. Any opinions, findings, and conclusions or recommendations expressed in this material are those of the authors and do not necessarily reflect the views of the National Science Foundation.

#### **ACKNOWLEDGMENTS**

This work is supported by the National Science Foundation, (DMR-1707859), and was facilitated by the IR/D (Individual Research and Development) program associated with AJH's appointment at the National Science Foundation.

## LITERATURE CITED

- Skoog DA. Principles of instrumental analysis. Cengage Learning, Australia, seventh edition. edition, 2018 - 2007.
- McCreery RL. Magnitude of Raman Scattering, chapter 2, pages 15–33. John Wiley & Sons, Ltd, 2000.
- 3. Takahashi M, Niwa M, and Ito M. Vibrational frequency shifts of adsorbed pyridazine on a silver electrode studied by SERS. *J. Phys. Chem*, 91(1):11–14, 1987.
- 4. Xi W, Shrestha BK, and Haes AJ. Promoting intra- and intermolecular interactions in surface-enhanced Raman scattering. *Analytical Chemistry*, 90(1):128–143, November 2017.
- Erasmus RM and Comins JD. Raman scattering. In Handbook of advanced nondestructive evaluation, pages 541–594. Springer International Publishing, 2019.
- 6. Quimby RS. Photonics and Lasers. John Wiley & Sons, Inc., March 2006.
- 7. Pilot, Signorini, Durante, Orian, Bhamidipati, and Fabris. A review on surface-enhanced Raman scattering. *Biosensors*, 9(2):57, April 2019.
- 8. Trivedi DJ, Barrow B, and Schatz GC. Understanding the chemical contribution to the enhancement mechanism in SERS: Connection with hammett parameters. *J. Chem. Phys.*, 153(12):124706, 2020.
- 9. Moskovits M. Persistent misconceptions regarding SERS. Phys. Chem. Chem. Phys., 15:5301–5311, 2013.

- Pierre MCS and Haes AJ. Purification implications on SERS activity of silica coated gold nanospheres. Anal. Chem., 84(18):7906-7911, 2012. PMID: 22924425.
- Phan HT and Haes AJ. What does nanoparticle stability mean? J. Phys. Chem. C, 123(27):16495–16507, May 2019.
- Jahn IJ, Mühlig A, and Cialla-May D. Application of molecular SERS nanosensors: where we stand and where we are headed towards? *Anal. Bioanal. Chem.*, 412(24):5999–6007, July 2020.
- Xu Y, Liu H, and Jiang T. Reliable quantitative SERS analysis mediated by Ag nano coix seeds with internal standard molecule. J Nanopart Res, 21(5), May 2019.
- Zhao F, Wang W, Zhong H, Yang F, Fu W, Ling W, and Zhang Z. Robust quantitative SERS analysis with relative Raman scattering intensities. *Talanta*, 221:121465, 2021.
- Zhang XQ, Li SX, Chen ZP, Chen Y, and Yu RQ. Quantitative SERS analysis based on multiple-internal-standard embedded core-shell nanoparticles and spectral shape deformation quantitative theory. Chemom. Intell. Lab. Syst., 177:47-54, 2018.
- Lorén A, Engelbrektsson J, Eliasson C, Josefson M, Abrahamsson J, Johansson M, and Abrahamsson K. Internal standard in surface-enhanced Raman spectroscopy. *Anal. Chem*, 76(24):7391–7395, 2004. PMID: 15595885.
- 17. Chio WIK, Davison G, Jones T, Liu J, Parkin IP, and Lee TC. Quantitative SERS detection of uric acid via formation of precise plasmonic nanojunctions within aggregates of gold nanoparticles and cucurbit[(n)]uril. J. Vis. Exp., 164, October 2020.
- Viehrig M, Rajendran ST, Sanger K, Schmidt MS, Alstrøm TS, Rindzevicius T, Zór K, and Boisen A. Quantitative SERS assay on a single chip enabled by electrochemically assisted regeneration: a method for detection of melamine in milk. *Anal. Chem*, 92(6):4317–4325, 2020. PMID: 31985206.
- Bell SEJ, Charron G, Cortés E, Kneipp J, de la Chapelle ML, Langer J, Procházka M, Tran V, and Schlücker S. Towards reliable and quantitative surface-enhanced Raman scattering (SERS): from key parameters to good analytical practice. Angew. Chem. Int. Ed., 59(14):5454–5462, 2020.
- Cialla-May D, Zheng XS, Weber K, and Popp J. Recent progress in surface-enhanced Raman spectroscopy for biological and biomedical applications: from cells to clinics. *Chem. Soc. Rev.*, 46:3945–3961, 2017.
- Shrestha BK and Haes AJ. Improving surface enhanced Raman signal reproducibility using gold-coated silver nanospheres encapsulated in silica membranes. J. Opt., 17(11):114017, oct 2015.
- Phan HT and Haes AJ. Impacts of pH and intermolecular interactions on surface-enhanced Raman scattering chemical enhancements. J. Phys. Chem. C, 122(26):14846–14856, 2018.
- Li L, Si Y, He B, and Li J. Au-Ag alloy/porous-SiO<sub>2</sub> core/shell nanoparticle-based surfaceenhanced Raman scattering nanoprobe for ratiometric imaging analysis of nitric oxide in living cells. *Talanta*, 205:120116, 2019.
- 24. Donoso-González O, Lodeiro L, Aliaga ÁE, Laguna-Bercero MA, Bollo S, Kogan MJ, Yutronic N, and Sierpe R. Functionalization of gold nanostars with cationic β-cyclodextrin-based polymer for drug co-loading and SERS monitoring. Pharmaceutics, 13(2), 2021.
- Oliveira MJ, P. de Almeida M, Nunes D, Fortunato E, Martins R, Pereira E, J. Byrne H, Águas H, and Franco R. Design and simple assembly of gold nanostar bioconjugates for surface-enhanced Raman spectroscopy immunoassays. *Nanomaterials*, 9(11), 2019.
- Shen W, Lin X, Jiang C, Li C, Lin H, Huang J, Wang S, Liu G, Yan X, Zhong Q, and Ren B. Reliable quantitative SERS analysis facilitated by core–shell nanoparticles with embedded internal standards. *Angew. Chem. Int. Ed.*, 54(25):7308–7312, 2015.
- Le Ru EC, Meyer SA, Artur C, Etchegoin PG, Grand J, Lang P, and Maurel F. Experimental demonstration of surface selection rules for SERS on flat metallic surfaces. *Chem. Commun.*, 47:3903–3905, 2011.

- 28. Harris DC and Bertolucci MD. Symmetry and spectroscopy: an introduction to vibrational and electronic spectroscopy. Dover Books on Chemistry Series. Dover Publications, 1989.
- Moskovits M and Suh JS. Surface selection rules for surface-enhanced Raman spectroscopy: calculations and application to the surface-enhanced Raman spectrum of phthalazine on silver. J. Phys. Chem. 88(23):5526-5530, 1984.
- 30. Kim J, Jang Y, Kim NJ, Kim H, Yi GC, Shin Y, Kim MH, and Yoon S. Study of chemical enhancement mechanism in non-plasmonic surface enhanced Raman spectroscopy (SERS). *Front. Chem.*, 7:582, 2019.
- 31. Wang X, Zhong J, Zhang M, Liu Z, Wu DY, and Ren B. Revealing intermolecular interaction and surface restructuring of an aromatic thiol assembling on Au(111) by tip-enhanced Raman spectroscopy. *J. Anal. Chem*, 88(1):915–921, 2016. PMID: 26633597.
- 32. Xi W and Haes AJ. Elucidation of HEPES affinity to and structure on gold nanostars. J. Am. Chem. Soc., 141(9):4034–4042, 2019. PMID: 30722659.
- Zhao H, Fu H, Zhao T, Wang L, and Tan T. Fabrication of small-sized silver NPs/graphene sheets for high-quality surface-enhanced Raman scattering. J. Colloid Interface Sci., 375(1):30–34, 2012.
- 34. Lu G, Shrestha B, and Haes AJ. Importance of tilt angles of adsorbed aromatic molecules on nanoparticle rattle SERS substrates. *J. Phys. Chem. C*, 120(37):20759–20767, 2016.
- 35. Schatz GC and Van Duyne RP. Electromagnetic mechanism of surface-enhanced spectroscopy, chapter 1-5. American Cancer Society, 2006.
- Jensen L, Aikens CM, and Schatz GC. Electronic structure methods for studying surfaceenhanced Raman scattering. Chem. Soc. Rev., 37:1061–1073, 2008.
- Zhang Q, He L, Rani KK, Wu D, Han J, Chen Y, and Su W. Colorimetric detection of neomycin sulfate in tilapia based on plasmonic core—shell Au@PVP nanoparticles. Food Chem., 356:129612, 2021.
- 38. Wang Y, Enrico JQQ, Ono T, Maeki M, Tokeshi M, Isono T, Tajima K, Satoh T, Sato S, Miura Y, and Yamamoto T. Enhanced dispersion stability of gold nanoparticles by the physisorption of cyclic poly(ethylene glycol). *Nat. Commun*, 11(1), November 2020.
- Garcia-Hernandez C, Freese AK, Rodriguez-Mendez ML, and Wanekaya AK. In situ synthesis, stabilization and activity of protein-modified gold nanoparticles for biological applications. Biomater. Sci., 7:2511–2519, 2019.
- Phan HT, Heiderscheit TS, and Haes AJ. Understanding time-dependent surface-enhanced Raman scattering from gold nanosphere aggregates using collision theory. J. Phys. Chem. C, 124(26):14287–14296, June 2020.
- 41. Jiang J, Wang S, Deng H, Wu H, Chen J, and Liao J. Rapid and sensitive detection of uranyl ion with citrate-stabilized silver nanoparticles by the surface-enhanced Raman scattering technique. R. Soc. Open Sci., 5(11):181099, November 2018.
- 42. Lu G, Forbes TZ, and Haes AJ. SERS detection of uranyl using functionalized gold nanostars promoted by nanoparticle shape and size. *Analyst*, 141(17):5137–5143, 2016.
- Sperling RA and Parak WJ. Surface modification, functionalization and bioconjugation of colloidal inorganic nanoparticles. *Philos. Trans. R. Soc. A*, 368(1915):1333–1383, 2010.
- 44. Pérez-Jiménez AI, Lyu D, Lu Z, Liu G, and Ren B. Surface-enhanced Raman spectroscopy: benefits, trade-offs and future developments. *Chem. Sci.*, 11:4563–4577, 2020.
- 45. Xue Y, Li X, Li H, and Zhang W. Quantifying thiol-gold interactions towards the efficient strength control. *Nat. Commun*, 5(1), July 2014.
- Xi W, Phan HT, and Haes AJ. How to accurately predict solution-phase gold nanostar stability. Anal. Bioanal. Chem., 410(24):6113-6123, May 2018.
- 47. Moran CH, Rycenga M, Zhang Q, and Xia Y. Replacement of poly(vinyl pyrrolidone) by thiols: a systematic study of Ag nanocube functionalization by surface-enhanced Raman scattering. J. Phys. Chem. C, 115(44):21852–21857, October 2011.
- 48. Pierre MCS, Mackie PM, Roca M, and Haes AJ. Correlating molecular surface coverage and

- solution-phase nanoparticle concentration to surface-enhanced Raman scattering intensities. J. Phys. Chem. C, 115(38):18511–18517, 2011.
- Wiedemair J, Le TNL, van den Berg A, and Carlen ET. Surface-enhanced Raman spectroscopy of self-assembled monolayer conformation and spatial uniformity on silver surfaces. J. Phys. Chem. C, 118(22):11857–11868, 2014.
- Brewer SH, Glomm WR, Johnson MC, Knag MK, and Franzen S. Probing BSA binding to citrate-coated gold nanoparticles and surfaces. *Langmuir*, 21(20):9303–9307, September 2005.
- Wang Y, Ji W, Sui H, Kitahama Y, Ruan W, Ozaki Y, and Zhao B. Exploring the effect of intermolecular H-bonding: a study on charge-transfer contribution to surface-enhanced Raman scattering of p-mercaptobenzoic acid. J. Phys. Chem. C, 118(19):10191-10197, 2014.
- Mosquera J, Zhao Y, Jang HJ, Xie N, Xu C, Kotov NA, and Liz-Marzán LM. Plasmonic nanoparticles with supramolecular recognition. Adv. Funct. Mater., 30(2):1902082, May 2019.
- Lu G, Forbes TZ, and Haes AJ. SERS detection of uranyl using functionalized gold nanostars promoted by nanoparticle shape and size. Analyst, 141:5137–5143, 2016.
- Phan HT, Geng S, and Haes AJ. Microporous silica membranes promote plasmonic nanoparticle stability for SERS detection of uranyl. Nanoscale, 12:23700-23708, 2020.
- Lu G, Johns AJ, Neupane B, Phan HT, Cwiertny DM, Forbes TZ, and Haes AJ. Matrix-independent surface-enhanced Raman scattering detection of uranyl using electrospun amidoximated polyacrylonitrile mats and gold nanostars. *Anal. Chem.*, 90(11):6766–6772, 2018. PMID: 29741873.
- Xi W and Haes AJ. Elucidation of pH impacts on monosubstituted benzene derivatives using normal Raman and surface-enhanced Raman scattering. J. Chem. Phys., 153(18):184707, 2020.
- 57. Huang L, Tang F, Shen J, Hu B, Meng Q, and Yu T. A simple method for measuring the SERS spectra of water-insoluble organic compounds. *Vib. Spectrosc.*, 26(1):15–22, 2001.
- Mukherjee KM and Misra NT. Solvent effect on surface-enhanced Raman activity of copperphthalocyanine on colloidal silver. Colloid and Surface B, 17(3):139–143, 2000.
- Lu G, Haes AJ, and Forbes TZ. Detection and identification of solids, surfaces, and solutions of uranium using vibrational spectroscopy. Coord. Chem. Rev., 374:314–344, 2018.
- 60. Hidi IJ, Heidler J, Weber K, Cialla-May D, and Popp J. Ciprofloxacin: pH-dependent SERS signal and its detection in spiked river water using LoC-SERS. *Anal. Bioanal. Chem.*, 408(29):8393–8401, October 2016.
- 61. Suryanarayana C. Nanocrystalline materials. Int. Mater. Rev., 40(2):41-64, 1995.
- 62. Shi H, Bi H, Yao B, and Zhang L. Dissolution of Au nanoparticles in hydrochloric acid solution as studied by optical absorption. Appl. Surf. Sci., 161(1):276–278, 2000.
- Tripathy SK, Woo JY, and Han CS. Highly selective colorimetric detection of hydrochloric acid using unlabeled gold nanoparticles and an oxidizing agent. *Anal. Chem.*, 83(24):9206–9212, 2011. PMID: 22074405.
- Wang F, He C, Han MY, Wu JH, and Xu GQ. Chemical controlled reversible gold nanoparticles dissolution and reconstruction at room-temperature. Chem. Commun., 48:6136–6138, 2012.
- 65. Xing W, Yin M, Lv Q, Hu Y, Liu C, and Zhang J. 1 oxygen solubility, diffusion coefficient, and solution viscosity. In Xing W, Yin G, and Zhang J, editors, Rotating electrode methods and oxygen reduction electrocatalysts, pages 1–31. Elsevier, Amsterdam, 2014.
- Sato T, Hamada Y, Sumikawa M, Araki S, and Yamamoto H. Solubility of oxygen in organic solvents and calculation of the Hansen solubility parameters of oxygen. *Ind. Eng. Chem. Res.*, 53(49):19331–19337, 2014.
- 67. Matikainen A, Nuutinen T, Itkonen T, Heinilehto S, Puustinen J, Hiltunen J, Lappalainen J, Karioja P, and Vahimaa P. Atmospheric oxidation and carbon contamination of silver and its effect on surface-enhanced Raman spectroscopy (SERS). Sci. Rep, 6(1), November 2016.
- Han Y, Lupitskyy R, Chou TM, Stafford CM, Du H, and Sukhishvili S. Effect of oxidation on surface-enhanced Raman scattering activity of silver nanoparticles: a quantitative correlation.

- Anal. Chem., 83(15):5873-5880, 2011. PMID: 21644591.
- 69. Jardón-Maximino N, Pérez-Alvarez M, Sierra-Ávila S, Ávila-Orta CA, Jiménez-Regalado E, Bello AM, González-Morones P, and Cadenas-Pliego G. Oxidation of copper nanoparticles protected with different coatings and stored under ambient conditions. J. Nanomater., 2018:1–8, September 2018.
- Nam J, Won N, Jin H, Chung H, and Kim S. pH-induced aggregation of gold nanoparticles for photothermal cancer therapy. J. Am. Chem. Soc, 131(38):13639–13645, 2009. PMID: 19772360.
- Tang B, Xu S, An J, Zhao B, Xu W, and Lombardi JR. Kinetic effects of halide ions on the morphological evolution of silver nanoplates. *Phys. Chem. Chem. Phys.*, 11:10286–10292, 2009.
- Kedia A and Kumar PS. Halide ion induced tuning and self-organization of gold nanostars. RSC Adv., 4:4782–4790, 2014.
- Zhang Z, Li H, Zhang F, Wu Y, Guo Z, Zhou L, and Li J. Investigation of halide-induced aggregation of Au nanoparticles into spongelike gold. *Langmuir*, 30(10):2648–2659, 2014. PMID: 24552456
- Christau S, Moeller T, Genzer J, Koehler R, and von Klitzing R. Salt-induced aggregation of negatively charged gold nanoparticles confined in a polymer brush matrix. *Macromolecules*, 50(18):7333-7343, 2017.
- 75. Xu X, Ji J, Chen P, Wu J, Jin Y, Zhang L, and Du S. Salt-induced gold nanoparticles aggregation lights up fluorescence of DNA-silver nanoclusters to monitor dual cancer markers carcinoembryonic antigen and carbohydrate antigen 125. Anal. Chim. Acta, 1125:41–49, 2020.
- Sun L, Song Y, Wang L, Guo C, Sun Y, Liu Z, and Li Z. Ethanol-induced formation of silver nanoparticle aggregates for highly active SERS substrates and application in DNA detection. J. Phys. Chem. C, 112(5):1415–1422, 2008.
- Wei H, Willner MR, Marr LC, and Vikesland PJ. Highly stable SERS pH nanoprobes produced by co-solvent controlled AuNP aggregation. Analyst, 141:5159–5169, 2016.
- 78. Han M, Lu H, and Zhang Z. Fast and low-cost surface-enhanced Raman scattering (SERS) method for on-site detection of flumetsulam in wheat. *Molecules*, 25(20), 2020.
- 79. Liu F, Gu H, Yuan X, Lin Y, and Dong X. Chloride ion-dependent surface-enhanced Raman scattering study of biotin on the silver surface. *J. Phys. Conf. Ser.*, 277:012025, jan 2011.
- 80. Zeng F, Xu D, Zhan C, Liang C, Zhao W, Zhang J, Feng H, and Ma X. Surfactant-free synthesis of graphene oxide coated silver nanoparticles for SERS biosensing and intracellular drug delivery. ACS Appl. Nano Mater., 1(6):2748–2753, 2018.
- 81. Kumar J and Thomas KG. Probing the bilayer-monolayer switching of capping agents on Au nanorods and its interaction with guest molecules. *J. Chem. Sci.*, 130(10), September 2018.
- Cheng Y, Zhao L, and Li T. Dendrimer-surfactant interactions. Soft Matter, 10:2714–2727, 2014.
- Doneux T. and De Decker Y. A simple model to describe the effect of electrostatic interactions on the composition of mixed self-assembled monolayers. *Langmuir*, 25(4):2199–2203, 2009.
   PMID: 19133814.
- 84. Volkert AA, Subramaniam V, Ivanov MR, Goodman AM, and Haes AJ. Salt-mediated self-assembly of thioctic acid on gold nanoparticles. *ACS Nano*, 5(6):4570–4580, 2011. PMID: 21524135.
- 85. West RM. Review—electrical manipulation of DNA self-assembled monolayers: electrochemical melting of surface-bound DNA. *J. Electrochem. Soc.*, 167(3):037544, January 2020.
- Chung T, Lee SY, Song EY, Chun H, and Lee B. Plasmonic nanostructures for nano-scale bio-sensing. Sensors, 11(11):10907–10929, 2011.
- 87. Etchegoin PG and Le Ru EC. A perspective on single molecule SERS: current status and future challenges. *Phys. Chem. Chem. Phys.*, 10:6079–6089, 2008.
- 88. Zhang W, Cui X, and Martin OJF. Local field enhancement of an infinite conical metal tip

- illuminated by a focused beam. J Raman Spectrosc, 40(10):1338–1342, 2009.
- Gersten J and Nitzan A. Electromagnetic theory of enhanced Raman scattering by molecules adsorbed on rough surfaces. J. Chem. Phys., 73(7):3023–3037, 1980.
- Lal S, Grady NK, Goodrich GP, and Halas NJ. Profiling the near field of a plasmonic nanoparticle with Raman-based molecular rulers. Nano Lett., 6(10):2338–2343, 2006. PMID: 17034107.
- 91. Maher RC. Raman spectroscopy for nanomaterials characterization · SERS hot spots: Datasheet from · volume : "Raman spectroscopy for nanomaterials characterization" in springermaterials (https://doi.org/10.1007/978-3-642-20620-7\_10). Copyright 2012 Springer-Verlag Berlin Heidelberg.
- Jain PK, Huang W, and El-Sayed MA. On the universal scaling behavior of the distance decay of plasmon coupling in metal nanoparticle pairs: a plasmon ruler equation. *Nano Lett.*, 7(7):2080–2088, 2007.
- 93. Mao L, Li Z, Wu B, and Xu H. Effects of quantum tunneling in metal nanogap on surface-enhanced Raman scattering. *Appl. Phys. Lett*, 94(24):243102, 2009.
- 94. Phan HT, Vinson C, and Haes AJ. Gold nanostar spatial distribution impacts the surface-enhanced Raman scattering detection of uranyl on amidoximated polymers. *Langmuir*, 37(16):4891–4899, 2021. PMID: 33861606.
- 95. Cho ES, Kim J, Tejerina B, Hermans TM, Jiang H, Nakanishi H, Yu M, Patashinski A, Glotzer SC, Stellacci F, and Grzybowski BA. Ultrasensitive detection of toxic cations through changes in the tunnelling current across films of striped nanoparticles. *Nat. Mater*, 11(11):978–985, September 2012.
- Li M, Qiu Y, Fan C, Cui K, Zhang Y, and Xiao Z. Design of SERS nanoprobes for Raman imaging: materials, critical factors and architectures. *Acta Pharm. Sin. B.*, 8(3):381–389, 2018.
- 97. Malinsky MD, Kelly KL, Schatz GC, and Van Duyne RP. Chain length dependence and sensing capabilities of the localized surface plasmon resonance of silver nanoparticles chemically modified with alkanethiol self-assembled monolayers. JACS, 123(7):1471–1482, 2001.
- Doering WE and Nie S. Spectroscopic tags using dye-embedded nanoparticles and surfaceenhanced Raman scattering. Anal. Chem, 75(22):6171-6176, 2003. PMID: 14615997.
- Shah KW, Sreethawong T, Liu SH, Zhang SY, Tan LS, and Han MY. Aqueous route to facile, efficient and functional silica coating of metal nanoparticles at room temperature. *Nanoscale*, 6:11273–11281, 2014.
- 100. England CG, Huang JS, James KT, Zhang G, Gobin AM, and Frieboes HB. Detection of phosphatidylcholine-coated gold nanoparticles in orthotopic pancreatic adenocarcinoma using hyperspectral imaging. *PLOS ONE*, 10(6):1–18, 06 2015.
- 101. Qian X, Peng XH, Ansari DO, Yin-Goen Q, Chen GZ, Shin DM, Yang L, Young AN, Wang MD, and Nie S. In vivo tumor targeting and spectroscopic detection with surface-enhanced Raman nanoparticle tags. Nat. Biotechnol, 26(1):83–90, December 2007.
- 102. Capocefalo A, Mammucari D, Brasili F, Fasolato C, Bordi F, Postorino P, and Domenici F. Exploring the potentiality of a SERS-active pH nano-biosensor. Front. Chem., 7:413, 2019.
- Ansar SM, Chakraborty S, and Kitchens CL. pH-responsive mercaptoundecanoic acid functionalized gold nanoparticles and applications in catalysis. *Nanomaterials*, 8(5), 2018.
- 104. Hu D, Li H, Wang B, Ye Z, Lei W, Jia F, Jin Q, Ren KF, and Ji J. Surface-adaptive gold nanoparticles with effective adherence and enhanced photothermal ablation of methicillinresistant staphylococcus aureus biofilm. ACS Nano, 11(9):9330–9339, 2017. PMID: 28806528.
- Häbel H, Särkkä A, Rudemo M, Blomqvist CH, Olsson E, and Nordin M. Colloidal particle aggregation in three dimensions. J. Microsc., 275(3):149–158, 2019.
- 106. Fraire JC, Pérez LA, and Coronado EA. Cluster size effects in the surface-enhanced Raman scattering response of Ag and Au nanoparticle aggregates: experimental and theoretical insight. J. Phys. Chem. C, 117(44):23090–23107, 2013.
- 107. Indrasekara DS, Swarnapali A, Thomas R, and Fabris L. Plasmonic properties of regiospe-

- cific core–satellite assemblies of gold nanostars and nanospheres. Phys. Chem. Chem. Phys.,  $17:21133-21142,\ 2015.$
- 108. Hernández Montoto A, Montes R, Samadi A, Gorbe M, Terrés JM, Cao-Milán R, Aznar E, Ibañez J, Masot R, Marcos MD, Orzáez M, Sancenón F, Oddershede LB, and Martínez-Máñez R. Gold nanostars coated with mesoporous silica are effective and nontoxic photothermal agents capable of gate keeping and laser-induced drug release. ACS Appl. Mater. Interfaces, 10(33):27644–27656, 2018. PMID: 30040374.
- 109. Atta S, Rangan S, and Fabris L. Highly tunable growth and etching of silica shells on surfactant-free gold nanostars. *ChemNanoMat*, 6(1):53–57, 2020.
- Harder RA, Wijenayaka LA, Phan HT, and Haes AJ. Tuning gold nanostar morphology for the SERS detection of uranyl. J Raman Spectrosc, 52(2):497–505, 2021.
- 111. Chegel VI, Naum OM, Lopatynskyi AM, and Lytvyn VK. Plasmonic nanochips for application in surface-enhanced fluorescence spectroscopy: factor of dielectric substrate. In Olena Fesenko and Leonid Yatsenko, editors, Nanoplasmonics, Nano-Optics, Nanocomposites, and Surface Studies, pages 395–412, Cham, 2015. Springer International Publishing.
- 112. Zhu J, Gao J, Li JJ, and Zhao JW. Improve the surface-enhanced Raman scattering from rhodamine 6g adsorbed gold nanostars with vimineous branches. Appl Surf Sci, 322:136–142, 2014.